International Journal of GEOMATE, May, 2017, Vol.12, Issue 33, pp. 114-121
Geotec., Const. Mat. & Env., ISSN:2186-2990, Japan, DOI: http://dx.doi.org/10.21660/2017.33.2641

ASSESSING TEMPORAL MOMENT CHARACTERISTICS OF SOLUTE TRANSPORT PHENOMENA IN HETEROGENEOUS AQUIFERS USING RANDOM WALK PARTICLE TRACKING

Yasuteru Kobi[1], *Kazuya Inoue[1] and Tsutomu Tanaka[1]

[1] Graduate School of Agricultural Science, Kobe University, Japan

*Corresponding Author, Received: 13 June 2016, Revised: 08 August 2016, Accepted: 30 Nov. 2016

ABSTRACT: Solute transport phenomenon is one of the crucial issues in predicting and spreading of a contaminant plume in natural aquifers. In this study, conservative solute transport simulations were conducted in two-dimensional heterogeneous aquifers to assess the transitional development of temporal moment characteristics up to the fourth order associated with macrodispersion phenomena. The aquifer system investigated here relied on the hydrogeologic data in the southwest of the Netherlands and was modeled as the heterogeneous aquifer with a certain geometric variance. Three types of physical heterogeneities in subsurface materials were represented as randomly correlated hydraulic conductivity fields, which were geostatistically generated under the isotropic assumption of the correlation length. Random walk particle tracking linked with temporal moment approach, which was based on observed breakthrough curves at several predefined control planes, demonstrated asymptotic variations of the second and fourth moments. Results also showed that the degree of the physical heterogeneity affected the degree of the increase of each moment, indicating that this plume behavior reflected the hydraulic conductivity distribution on which the evolution of plume was considerably dependent.

Keywords: Temporal Moment Characteristics, Solute Transport, Random Walk Particle Tracking, Heterogeneous Aquifers

1. INTRODUCTION

The mechanisms of spreading and mixing of solute in aquifers are strongly related to the heterogeneity associated with the hydraulic conductivity distribution. The behavior of groundwater contaminants such as salts and organic compounds is difficult to predict, is described as a complex function of space and time in terms of advection by the random velocity field and pore-scale dispersion and can be viewed as a spreading of particle cloud [1]. Inherently, the position of the center of particle cloud can be reliably computed because it depends on the mean seepage velocity of groundwater flow, which is observed in a field. On the other hand, the degree of the elongation of the particle cloud around the central position along each orthogonal axis is a more elusive variable due to dispersion processes, especially in heterogeneous aquifers [2].

Heterogeneity causes enhanced advective spreading of the solute particle cloud which is a phenomenon referred to as macrodispersion [2][3]. In most groundwater aquifers, heterogeneous nature of hydraulic conductivity provides a wide variety of solute pathways at different velocities and governs the fate of solute transport. As for the future prediction of contamination, some remediation or cleanup strategies of contaminated groundwater and the framework of risk assessment associated with human health, hydrogeologic characterization in terms of the degree of the spatial variation in an aquifer is one of key issues [4].

As well as the development of the theory of flow through porous media, some of the efforts made to understand better macrodispersion phenomena have been conducted through theoretical, experimental and numerical studies [5]-[10]. Several physical and mathematical models for sorbing or desorbing solute transport in heterogeneous aquifers associated with the retardation factor or the distribution coefficient have been developed. Especially, a negative correlation relation between the hydraulic conductivity and the distribution coefficient is a representative model expressing solute spreading under the sorptive condition [11]-[13]. However, macrodispersion and relevant statistical moments do not provide information about the actual distribution of particle crowd. Ideally, the Gaussian or non-Gaussian features of the growth of spreading of particle cloud should be assessed for a practical use of the findings. This paper attempts to provide additional evidence related to conservative solute spreading in heterogeneous aquifers by performing numerical experiments under controlled conditions.

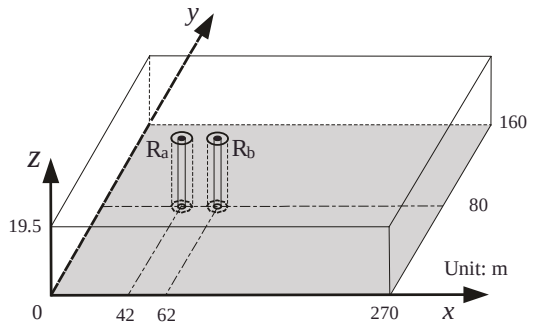

Fig.1 Schematic drawing of the model domain adopted in this study.

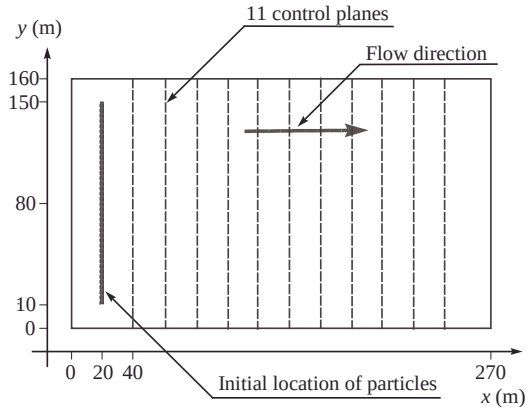

Fig. 2 Sketch of solute transport simulations showing the initial location of particles and the control planes.

The objective of this study is to assess the transitional development of moment characteristics up to the fourth order associated with macrodispersion phenomena in conservative solute transport simulations. Based on the hydrogeologic data reported in the Netherlands, random walk particle tracking linked with temporal moment approach is carried out in two-dimensional heterogeneous aquifers. Numerical solute transport experiments are conducted in these aquifers under natural-gradient flow conditions for identifying the four statistical moments in terms of temporal moments of particle arrival times at prescribed control planes. Even with hypothetical sources of contamination in groundwater, the modeling studies shed some light on the complex pathways of contaminates in subsurface systems and the characteristics of solute transport phenomena.

2. PROBLEM DESCRIPTION

2.1 Site Description and Flow Set-up Configuration

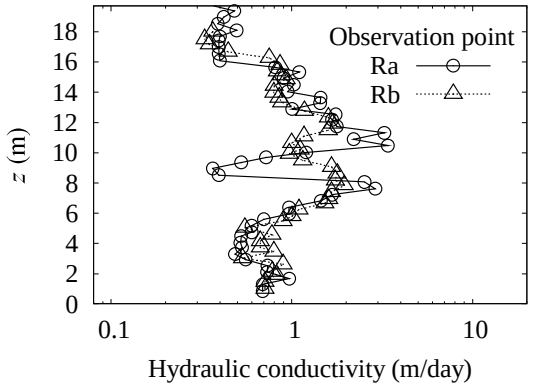

Fig. 3 Variation of hydraulic conductivity derived from granular analysis [14].

The disposal site of concern is located in the dunes near the Hague in the Netherlands. In 1984 a tracer test was conducted to mainly investigate the feasibility of artificial recharge by means of infiltration wells [14]. Solute transport simulations consider a three-dimensional confined aquifer with uniform flow in the *x*-direction driven by a mean hydraulic gradient equal to 0.005. The size of the flow domain adopted herein extends 270 m in the *x*-direction, 160 m in the *y*-direction and 19.5 m in the *z*-direction as shown Fig. 1. The domain size of interest both in *x* and *y* directions are relatively larger than that in the *z*-direction. Therefore, this study site was treated as a horizontally two-dimensional aquifer as shown Fig. 2. Notice that this site is not polluted any contaminants.

The hydraulic conductivity data employed in this study are based on the two vertical cores whose locations are shown as Ra and Rb in Fig.1. Hydraulic conductivity data derived by granular analysis of soil samples are given in Fig. 3 and also the porosity of the aquifer was assumed to be 0.35 [14]. In addition, the hydraulic conductivity and the degree of heterogeneity of this aquifer were set to 0.821 m/day and 0.151, respectively.

In this study, a two-dimensional, log-conductivity model with an isotropic exponential covariance function was used to generate 30 realizations of the hydraulic conductivity field using the block kriging with the correlation length of 13 m [15]. As a semi-variogram model, exponential model without the anisotropy was utilized. A few representative realizations showing the physical heterogeneity in terms of the hydraulic conductivity are exhibited in Fig. 4. In addition to the heterogeneity of 0.151, 0.5 and 1.0 of the geometric variance of hydraulic conductivity were employed as relatively higher heterogeneity and relevant 30 realizations were generated in the same manner using the block kriging.

For solute transport simulations, a saturated

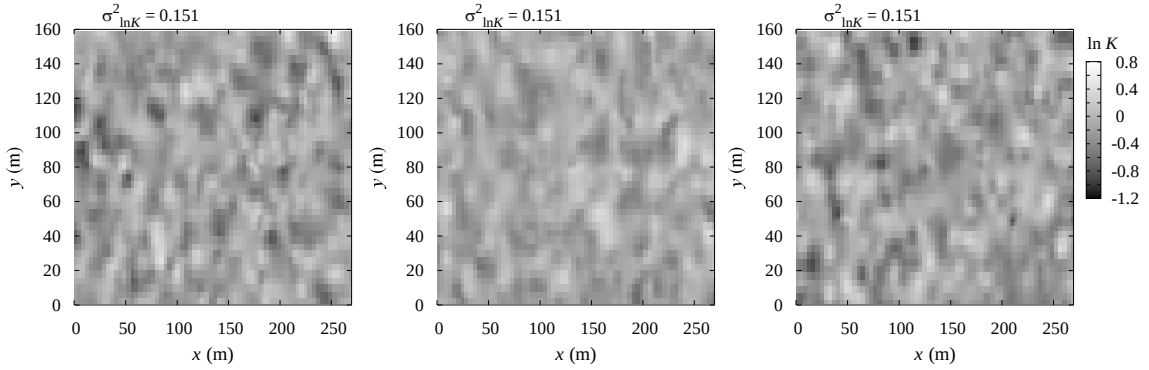

Fig. 4 Representative realizations of ln *K* field with the degree of heterogeneity of 0.151.

velocity field within a heterogeneous porous medium must initially be developed [16].

$$\nabla \cdot \left(K(\mathbf{x}) \nabla h \right) = 0 \tag{1}$$

where h is the hydraulic head at vector location, $K(\mathbf{x})$ is the hydraulic conductivity at location $\mathbf{x}$. Steady fluid flow in this system is described by the Darcy's law:

$$\mathbf{v}(\mathbf{x}) = -K(\mathbf{x}) \nabla h / n_p \tag{2}$$

where $\boldsymbol{v}$ is the pore velocity and n_p is the porosity. In this study, the porosity in this site is assumed to be equal to the effective porosity. The boundary condition of the Dirichlet type was specified on two sides faces intersecting the plane with x = 0 m (upstream side) and x = 270 m (downstream side), while other sides were treated as no-flow Neumann type boundaries. These boundary conditions provided the establishment of the mean hydraulic gradient of 0.005 and were linked with the finite element method for computing spatial distributions of the hydraulic head and seepage velocity.

2.2 Random Walk Particle Tracking

Particle tracking is a widely applied tool to investigate aquifer characteristics in groundwater flow models and to visualize groundwater injection and pumping from as wells and streams [17]-[19]. Random walk particle tracking (RWPT) is one of the particle tracking techniques and simulates solute transport by partitioning the solute mass into a large number of representative particles. The evolution in time of a particle is driven by a drift term that relates to the advective movement and a superposed Brownian motion responsible for dispersion [20], [21].

Numerical simulation of advective and dispersive mass transport in porous media may proceed over discrete time steps by moving the particles according to the explicit random walk particle tracking algorithm given as Ito interpretation of Langevin equation [14]:

$$\mathbf{X}_p(t+\Delta t) = \mathbf{X}_p(t) + \left(\mathbf{v} + \nabla \cdot \mathbf{D} \right) \Delta t + \mathbf{B} \boldsymbol{\Xi} \sqrt{\Delta t} \tag{3}$$

where $\mathbf{X}_p$ is the component of the particle location at time t, Δt is the time increment, $\boldsymbol{\Xi}$ is a vector which contains three normally distributed random numbers with zero mean and unit variance and $\mathbf{D}$ is the velocity-dependent dispersion tensor as follows [16]:

$$\begin{aligned} \mathbf{D} = & \left(\alpha_{TH} |\mathbf{v}| + \frac{v_3^2}{|\mathbf{v}|} \left(\alpha_{TV} - \alpha_{TH} \right) + D_d \right) \mathbf{I} \\ & + \left(\alpha_{TV} - \alpha_{TH} \right) \left(e_i e_j |\mathbf{v}| - \frac{v_3}{|\mathbf{v}|} \left(e_i v_j + e_j v_i \right) \right) \\ & + \left(\alpha_L - \alpha_{TH} \right) \frac{v_i v_j}{|\mathbf{v}|} \end{aligned} \tag{4}$$

where α_L is the longitudinal dispersivity, α_{TH} and α_{TV} are the horizontal and vertical transverse dispersivities, respectively, D_d is the diffusion coefficient, $\mathbf{I}$ is the unit matrix and e_i is the unit vector in the z-direction.

The displacement matrix $\mathbf{B}$ in the three-dimensional form represents the direction displacement distance for the random process [22],[23]

$$\mathbf{B} = \begin{pmatrix} \frac{v_1}{|\mathbf{v}|} \sqrt{2\alpha_L |\mathbf{v}|} & \frac{-v_1 \sqrt{J}}{\Gamma} & \frac{-v_1 v_3 \sqrt{2\alpha_{TV} |\mathbf{v}|}}{|\mathbf{v}| \Gamma} \\ \frac{v_2}{|\mathbf{v}|} \sqrt{2\alpha_L |\mathbf{v}|} & \frac{v_1 \sqrt{J}}{\Gamma} & \frac{-v_2 v_3 \sqrt{2\alpha_{TV} |\mathbf{v}|}}{|\mathbf{v}| \Gamma} \\ \frac{v_3}{|\mathbf{v}|} \sqrt{2\alpha_L |\mathbf{v}|} & 0 & \frac{\Gamma \sqrt{2\alpha_{TV} |\mathbf{v}|}}{|\mathbf{v}|} \end{pmatrix} \tag{5}$$

$$\Gamma = \sqrt{v_1^2 + v_2^2}, \; J = 2 \left(\frac{\alpha_{TH} \Gamma^2 + \alpha_{TV} v_3^2}{|\mathbf{v}|} \right) \tag{6}$$

Equilibrium sorption using a linear isotherm can be incorporated by replacing the velocity **v** with a retarded velocity **v**/*R* and **D** with **D**/*R* in Eq.(3) where *R* is the retardation factor.

2.3 Temporal Moment Analysis

Based on a mass assigned to each particle, temporal moments associated with observed breakthrough curves (BTCs) at prescribed control planes are able to be computed using particle passing time through control planes. An eminent feature of random walk particle tracking is the efficient estimation of temporal moments without calculating solute concentration at a certain location and having to evaluate an entire shape of BTCs [7]. The *n*th normalized absolute temporal moment was calculated as the expected value of the arrival time of a particle at the control plane to the *n*th power [7]:

$$M_{n,T} = \frac{1}{N_r}\sum_{r=1}^{N_r}\left(\sum_{k=1}^{NP_s} m_p^k \left(t_p^k(x_P)\right)^n \Big/ \sum_{k=1}^{NP_s} m_p^k\right)^{(r)} \tag{7}$$

where $M_{n,T}$ is the *n*th normalized absolute temporal moment, x_P is the mean flow direction coordinate, m^k_p is the mass assigned to the *k*th particle, t^k_p is the first arrival passage time of the *k*th particle, NP_s is the total number of particles arrived at the x_P-control plane, N_r is the total number of realizations and *r* with the brackets means the corresponding realization number. As shown in Eq.(7), ensemble of corresponding temporal moments was taken among all realizations.

The *n*th normalized central temporal moment is calculated using relationship between central and absolute temporal moments.

$$\Lambda_{n,T} = \sum_{r=0}^{n}\binom{n}{r} M_{n-r,T}(x_P)\left(-M_{1,T}(x_P)\right)^r \tag{8}$$

where $\Lambda_{n,T}$ is the *n*th normalized central temporal moment.

The third and the fourth central temporal moments can also be expressed by means of the coefficients of skewness and kurtosis, respectively, which measure the asymmetry and relative peakedness of the BTCs as compared with a Gaussian distribution [7]

$$C_S = \Lambda_{3,T} / \left[\Lambda_{2,T}\right]^{3/2} \tag{9}$$

$$C_K = \Lambda_{4,T} / \left[\Lambda_{2,T}\right]^2 - 3 \tag{10}$$

where is C_S is the skewness and C_K is the kurtosis. With the above definitions, a Gaussian BTC leads to zero skewness and kurtosis. Parameters used in this analysis are listed in Table 1.

Table 1 Parameters used in RWPT

Parameter	Description	Value
Random walk particle tracking		
NP (-)	Number of particles	20000
Δt (day)	Time step	1
Transport parameters		
α_L (m)	Longitudinal dispersivity	0.02
α_{TH} (m)	Transverse dispersivity	0.005
D_d (m^2/day)	Effective diffusion coefficient	0
R (-)	Retardation factor	1.0
J (-)	Hydraulic gradient	0.005
n_p (-)	Porosity	0.35
Heterogeneous flow field		
Model	Exponential	
λ (m)	Correlation length	13

3. RESULTS AND DISCUSSION

3.1 Random Walk Particle Tracking Implementations

In all simulations, RWPT algorithms stated above were repeatedly performed under the prescribed flow conditions while finite element model was the computational framework for expressing the velocity vector at all locations in the model domain. As an initial pulse input, the number of particles used to represent the solute crowd was set to 20000 with a constant mass of the unit gram per one particle. All particles were stochastically applied under the condition of the uniform distribution within the initial injection line shown in Fig. 2. Additionally, longitudinal dispersivity and transverse dispersivities were chosen to be 0.02 m and 0.005 m, respectively, which were based on the data reported in the literature [14]. To simplify the problem, a particle was assumed to be conservative and not to have the adsorptive nature, leading to 1 of the retardation factor.

Representative three results of mass BTCs divided by the total mass at three control planes

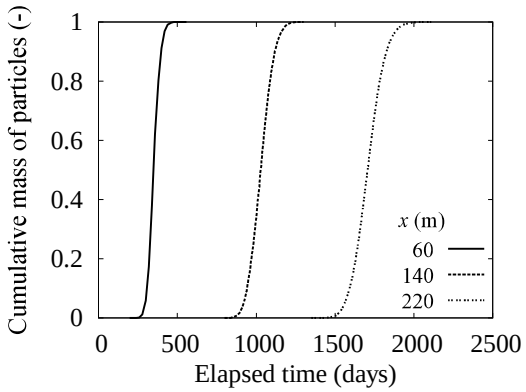

Fig. 5 Representative breakthrough curves measured at three control planes.

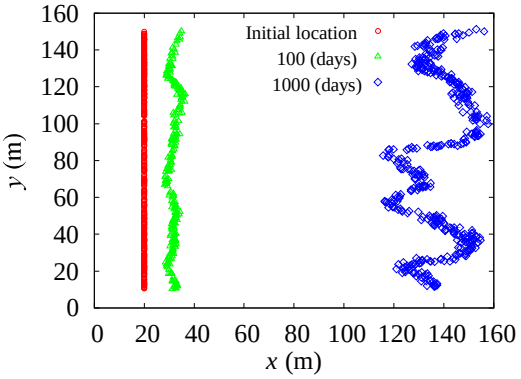

Fig. 6 Particle cloud distributions at initial (t=0), 100 and 1000 days. This figure is based on a single realization.

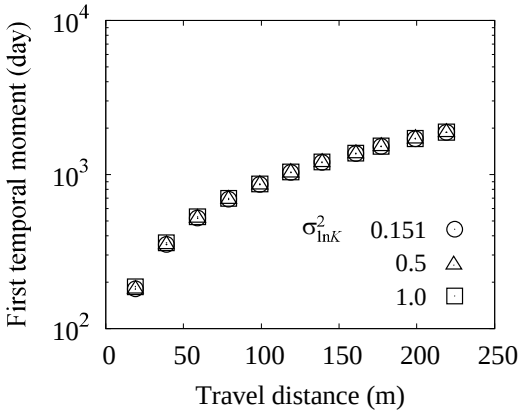

Fig. 7 Variation of the first-order temporal moments estimated from BTCs at 11 control planes.

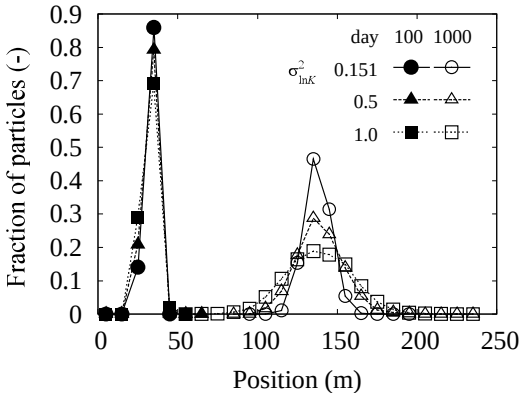

Fig. 8 Fraction of particle positions. Closed symbols are the fraction of particles at day=100 and open symbols are at day=1000.

are exhibited in Fig. 5. A time series mass variation at control planes indicates that breakthrough curves exhibit a Gaussian-like shape regardless of the location of a control plane. To visualize a particle cloud variation, particle clouds at different three times for a single realization are shown in Fig. 6. A line type source varies its distribution cloud according to the hydraulic conductivity distribution during the course of transport. The first to the fourth moments, which were taken as ensemble average values for all realizations, were assessed to elucidate the temporal moment characteristics in BTCs and the transport property in heterogeneous aquifers.

3.2 First-Order Temporal Moments

Ensemble of first-order temporal moments obtained from Eq.(7) and Eq.(8) for all realizations is shown in Fig. 7 as a function of the distance to the control plane from the source for different degrees of heterogeneity. The results of first temporal moments correspond to the mean arrival time of solute particles during the migration, demonstrating that the degree of heterogeneity little influences on the mean arrival time. In order to visualize this point, the fraction of particle positions along x-direction at elapsed times t=100 and 1000 days after the particle release is depicted in Fig. 8. In this figure, all distributed particles in the entire domain were projected onto the x-axis and were counted with the interval of 10 m according to the particle locations. The positions of the peak of the fraction are almost identical despite of the degree of heterogeneity, indicating the validity of the outcomes of the first-order temporal moments. Also, the variation of the fraction of particle exhibits the difference of the absolute values of the fraction of particle and depends on the degree of heterogeneity. The difference of the peak values attributes to the solute transport nature as the degree of solute spreading increases with the increase of the heterogeneity. This point leads to

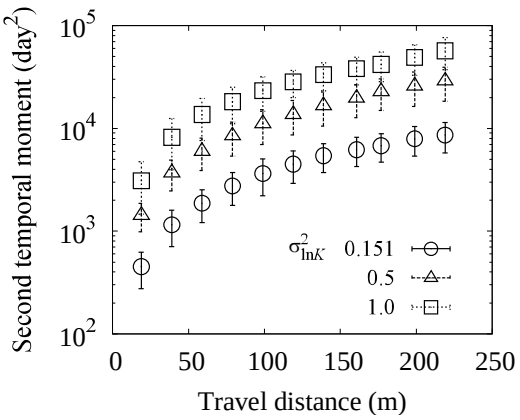

Fig. 9 Results of the second-order temporal moments estimated from ensemble average BTCs at 11 control planes in three aquifers with different heterogeneities.

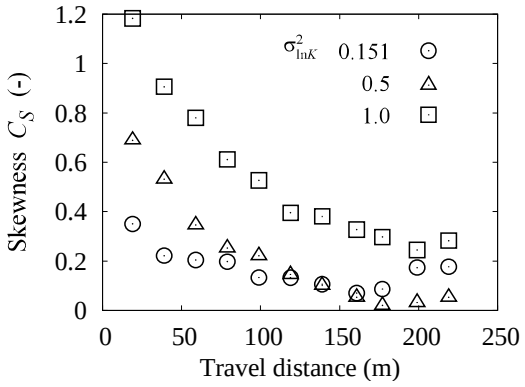

Fig. 10 Results of the skewness of ensemble average BTCs as a function of travel distance in three aquifers with different heterogeneities.

the difference of the macrodispersion phenomena in heterogeneous porous media [3],[9].

3.3 Second-Order Temporal Moments

Figure 9 provides the results of the second-order temporal moments, which are used to gauge the size of a particle cloud in a given direction and determine the rate of growth with the increase of the transport displacement. In this figure, the error bars are illustrated to show the variance of ensemble of all realizations. It can be seen that values of the second-order temporal moments increase nonlinearly in all heterogeneities while the magnitude of the variance shown as bars remains almost constant during the transport.

At large travel distance, second-order temporal moments gradually approach certain values whereas an asymptotic value depends on the degree of heterogeneity. As aforementioned above, the difference of the absolute values of second-order temporal moments results in the difference of the degree of macrodispersion. Moreover, the larger the values of second-order temporal moments grow, the larger likely the outcomes of macrodispersivity become [10],[24],[25].

3.4 Third-Order Temporal Moments

The approach of temporal moments is an efficient tool for characterizing solute transport, especially in high-order temporal moments due to long tails of the BTC with small concentrations. The study of third and fourth moments of BTCs is a crucial step toward characterizing the shape of the BTC not only Gaussian but non-Gaussian [25],[26]. RWPT can provide accurate estimates of the third and fourth central temporal moments under the influence of heterogeneity of BTCs. Results are expressed by means of the skewness and kurtosis, which measure the asymmetry and peakedness of the BTCs, respectively.

The results of the skewness estimated from ensemble average BTCs as a function of travel distance of particle cloud are plotted in Figure 10. At small travel distances, the decrease rate is fast as pointed out by Fernàndez-Garcia et al. [7]. The values of the skewness decrease with the increase of travel distance and approach the value of zero or non-zero. This may attribute the Wiener process of Eq.(3) in terms of Ito interpretation and Markov process where future movement of a particle depends only on where the particle is, not the history of particle transport pathways. However, non-zero nature of the skewness values under the travel distance of interest appears to be persistent. Moreover, somewhat fluctuation of values at a relatively large distance occurs, suggesting the need in terms of a longer transport phenomenon under the larger correlation scales in heterogeneous aquifers.

3.5 Fourth-Order Temporal Moments

Figure 11 presents the variation of the kurtosis as a function of travel distance from the source estimated from ensemble average BTCs. Kurtosis expresses the relative peakedness or flatness of a distribution relative to a normal distribution where positive values indicate a relatively peaked distribution. The values of the kurtosis of the BTCs decrease with the increase of travel distance, leading to a Gaussian-like particle distribution. Like the results of skewness shown in Fig. 10, at small distances, the larger decrease appears and gradually dissipates over the course of travel

distances. This tendency agrees with earlier work [7], suggesting the reliability of estimates.

It is interesting to note that although these deviations in skewness and kurtosis from the values corresponding to a Gaussian distribution increase with the increase of the heterogeneity, the influence of the degree of heterogeneity on the evolution of the kurtosis coefficient gradually dissipates at larger travel distances. This point is similar to the results of the third temporal moments.

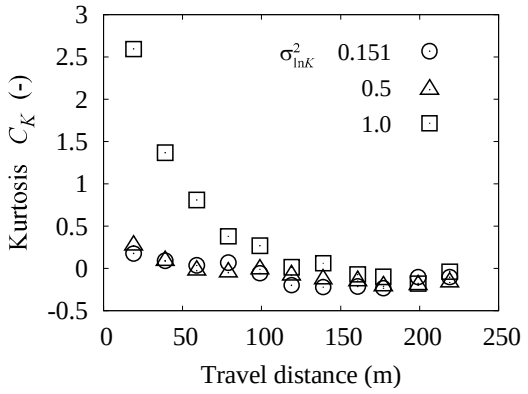

Fig. 11 Results of the kurtosis of ensemble average BTCs as a function of travel distance in three aquifers with different heterogeneities.

4. CONCLUSION

In this study, temporal moment characteristics associated with conservative solute transport phenomena in heterogeneous two-dimensional aquifers were evaluated using the random walk particle tracking linked with the temporal moment approach. The following findings have been clarified.

1. Non-dependency of the mean arrival times on the degree of heterogeneity was confirmed through the result of first-order temporal moments.
2. The values of the second-order temporal moment approach a constant value according to the degree of heterogeneity.
3. It was observed that skewness and kurtosis decrease with the increase of the travel distance. This point reflects that the shape of the distribution of the particles become Gaussian-like shape far away from the source.

In natural aquifers, the system strives to attain equilibrium between adsorbed and desorbed phases referred to as sorption. A nonlinear evolution of particle cloud and a long tailing of BTC may be of importance to significantly characterize the sorptive particle transport phenomena.

5. ACKNOWLEDGEMENTS

Part of this study was funded by JSPS (16K07941).

6. REFERENCES

[1] Dagan G, “Solute transport in heterogeneous porous formations”, J. Fluid Mech., 145, 1984, pp.151-177.

[2] Dagan G, Fiori A, “The influence of pore-scale dispersion on concentration statistical moments in transport through heterogeneous aquifers”, Water Resour. Res., 33(7), 1997, pp.1595-1605.

[3] Gelhar LW, Welty C, Rehfeldt KW, “A critical review of data on field-scale dispersion in aquifers”, Water Resour. Res., 28(7), 1992, pp.1955-1974.

[4] Kitanidis PK, “Prediction by the method of moments in a heterogeneous formation”, J. Hydrol., 102, 1988, pp.453-473.

[5] Dagan G, “Theory of solute transport by groundwater”, J. Fluid Mech., 145, 1984, pp.151-177.

[6] McNeil JD, Oldenborger GA, Schincariol RA, “Quantitative imaging of contaminant distributions in heterogeneous porous media laboratory experiments”, J. Contam. Hydrol., 84, 2006, pp.36-54.

[7] Fernàndez-Garcia D, Illangasekare TH, Rajaram H, “Difference in the scale-dependence of dispersivity estimated from temporal and spatial moments in chemically and physically heterogeneous porous media”, Adv. Water Resour, 28, 2005, pp.745-759.

[8] Beaudoin A, de Dreuzy J-R, “Numerical assessment of 3-D macrodispersion in heterogeneous porous media”, Water Resour. Res., 49, 2013, pp.2489-2496.

[9] Inoue K, Fujiwara T, Kurasawa T, Tanaka T, “Quantification of solute macrodispersion phenomena and local heterogeneity using intermediate-scale solute transport experiments in heterogeneous porous formations”, J. JSCE A(2), 70(2), 2015, pp.691-702 (in Japanese) .

[10] Inoue K, Fujiwara T, Tanaka T, “Identifying solute dispersivity in unsaturated porous media using a non-intrusive technique”, Inter. J. GEOMATE, 5, 2013, pp.743-748.

[11] Chrysikopoulos CV, Kitanidis PK, Roberts PV, “Macrodispersion of sorbing solute in heterogeneous porous formations with spatially periodic retardation factor and

velocity field", Water Resour. Res., 28(6), 1992, pp.1517-1529.
[12] Robin MJL, Sudicky EA, Gillham RW Kachanoski RG, "Spatial variability of strontium distribution coefficients and their correlation with hydraulic conductivity in the Canadian forces base Borden aquifer", Water Resour. Res., 27(10), 1991, pp.2619–2632.
[13] Fernàndez-Garcia D, Illangasekare TH, Rajaram H, "Conservative and sorptive forced-gradient and uniform flow tracer tests in a three-dimensional laboratory test aquifer", Water Resour. Res., 40, 2004, W10103.
[14] Uffink GJM, "Analysis of dispersion by the random walk method", Ph.D. Dissertation, Delft University of Technology, 1990, 150p.
[15] Deutsch, CV, Journel AG, "GSLIB: Geostatistical software library and user's guide", Oxford University Press, 1992, 340p.
[16] Bear J, "Dynamics of fluids in porous media**"**, Dover Publications, 1972, 764p.
[17] Pint CD, Hunt RJ, Anderson MP, "Flowpath delineation and ground water age, Allequash Basin, Wisconsin", Groundwater, 41, 2003, pp.895–902, doi:10.1111/j.1745-6584.2003.tb02432.x.
[18] Sanford W, "Calibration of models using groundwater age", Hydrogeol. J., 19, 2010, pp.13–16, doi:10.1007/s10040-010-0637-6.
[19] McDonnell JJ, McGuire K, Aggarwal P, Beven K, Biondi D, Destouni G, Dunn S, James A, Kirchner J, Kraft P, Lyon S, Małoszewski P, Newman B, Pfister L, Rinaldo A, Rodhe A, Sayama T, Seibert J, Solomon K, Soulsby C, Stewart M, Tetzlaff D, Tobin C, Troch P, Weiler M, Western A, Wörman A, Wrede S, "How old is streamwater? Open questions in catchment transit time conceptualization, modelling and analysis", 24, 2010, Hydrol. Process., pp.1745–1754, doi:10.1002/hyp.7796.
[20] Tompson AFB, Gelhar LW, "Numerical simulation of solute transport in three-dimensional, randomly heterogeneous porous media", Water Resour. Res., 26, 1990, pp.2541-2562.
[21] Salamon P, Fernàndez-Garcia D, Gomez-Hernàndez JJ, "A review and numerical assessment of the random walk particle tracking method", J. Hydrol., 87(1-4), 2006, pp.277-305.
[22] Lichtner PC, Kelkar S, Robinson B, "New form of dispersion tensor for axisymmetric porous media with implementation in particle tracking", Water Resour. Res., 38, 2002, pp.21-1-21-16.
[23] Inoue K, Tanaka T, "Random walk particle tracking approach to assess 3-d macrodispersion in heterogeneous aquifers", Proceedings of the 15th Asian Regional Conference on Soil Mechanics and Geotechnical Engineering, 2015, pp.685-690.
[24] Fernàndez-Garcia D, Rajaram H, Illangasekare TH, "Assessment of the predictive capabilities of stochastic theories in a three-dimensional laboratory test aquifer: Effective hydraulic conductivity and temporal moments of breakthrough curves", Water Resour. Res., 41, 2005, W04002.
[25] Luo J, Cirpka OA, Dentz M, Carrera J, "Temporal moments for transport with mass transfer described by an arbitrary memory function in heterogeneous media", Water Resour. Res., 44, 2008, W01502.
[26] Inoue K, Kurasawa T, Tanaka T, "Quantification of macrodipsersion in laboratory-scale heterogeneous porous formations", Inter. J. GEOMATE, 10, 2016, pp.1854-1961.